

# Numerical Analysis of Spherical Wave Absorption by a Thin Metamaterial Absorber

Satoshi Yagitani, Naoya Fukuoka, Ryohei Hayashi, and Mitsunori Ozaki  
Kanazawa University, Kakuma-machi, Kanazawa 920-1192, Japan

**Abstract** – Absorption and reflection characteristics of a spherical wave incident on a metamaterial absorber are numerically calculated on the basis of the plane-wave expansion technique. The absorbed and reflected field and power distributions on the absorber surface can be rigorously evaluated for a spherical wave radiated from a nearby RF source.

**Index Terms** — Metamaterial absorber, Spherical wave, Plane-wave expansion, Reflection, Absorption.

## I. INTRODUCTION

A variety of thin electromagnetic wave absorbers have been realized with metamaterial structures working as artificial magnetic conductors (AMC) [1]. As a new application of such a metamaterial absorber, it was proposed that a mushroom-type structure could be used for monitoring 2-d field distributions of an incident RF wave [2], [3]. Lumped resistors interconnecting an array of surface patches were used to absorb the incident RF power, which was monitored by a 2-d array of power detectors attached to the resistors. The technique was validated by simulation and measurement.

When monitoring the power distribution nearby an RF source, the absorber is illuminated with a spherical wave. It is necessary to evaluate its absorption characteristics for the spherical-wave incidence in addition to the conventional plane-wave incidence. In this study, the absorption and reflection characteristics of a spherical wave by a metamaterial absorber are numerically calculated using plane-wave expansion of the spherical wave. Preliminary results are presented and discussed.

## II. CALCULATION MODEL AND PROCEDURE

The propagation of a spherical wave is evaluated with the calculation model illustrated in Fig. 1. A dipole transmitter along the z-direction is placed at the origin and radiates a spherical wave with a certain directionality. A thin metamaterial absorber placed on the  $xz$ -plane at a distance of  $y_a$  from the transmitter is illuminated with the spherical wave. On the absorber surface the 2-d electromagnetic field distribution of the spherical wave is expanded into a large number of plane waves using the Fourier analysis [4], as

$$\mathbf{E}(x, y_a, z) = \iint \mathbf{E}_p(k_x, y_a, k_z) \exp\{-j(k_x x + k_z z)\} dk_x dk_z, \quad (1)$$

where  $\mathbf{E}(x, y_a, z)$  represents the spatial distribution of electromagnetic field, and  $\mathbf{E}_p(k_x, y_a, k_z)$  denotes the electromagnetic field of elementary plane waves propagating in the direction of  $\mathbf{k}_0 = (k_x, k_y, k_z)$ , where  $k_y = \{k_0^2 - (k_x^2 + k_z^2)\}^{1/2}$ , where  $k_0$  is the wavenumber in free space. The reflection characteristics of the elementary plane waves can be calculated using the surface impedance of the metamaterial absorber. Here we use the metamaterial structure composed of an electrically dense array of square metal patches on the surface of a thin dielectric substrate with a grounding plane on the backside. The surface impedance of this type of structure is given by [5]

$$Z_s^{\text{TE}} = j\omega L_s / [1 - \omega^2 L_s C_s \{1 - \sin^2 \theta / (\epsilon_r + 1)\}], \quad (2)$$

$$Z_s^{\text{TM}} = j\omega L_s (1 - \sin^2 \theta / \epsilon_r) / \{1 - \omega^2 L_s C_s (1 - \sin^2 \theta / \epsilon_r)\}, \quad (3)$$

for TE and TM incidence, where  $L_s$  and  $C_s$  are the effective inductance and capacitance of the structure, which exhibits an AMC feature at the LC resonance frequency. Here  $\epsilon_r$  is the relative permittivity of the substrate and  $\theta$  is the angle of incidence. The absorption is achieved by the lumped resistors  $R$  inserted between the surface patches at the resonance frequency, which is made tunable with additional capacitors  $C$  as in the right panel in Fig. 1 [2]. The TE and TM reflection coefficients are calculated using (2) and (3), as

$$R^{\text{TE}} = (Z_s^{\text{TE}} // Z - \eta_0 / \cos \theta) / (Z_s^{\text{TE}} // Z + \eta_0 / \cos \theta), \quad (4)$$

$$R^{\text{TM}} = (Z_s^{\text{TM}} // Z - \eta_0 \cos \theta) / (Z_s^{\text{TM}} // Z + \eta_0 \cos \theta), \quad (5)$$

respectively, where  $\eta_0$  is the wave impedance in free space,  $Z = R \parallel 1/j\omega C$ , and  $\parallel$  means the parallel connection of impedance.

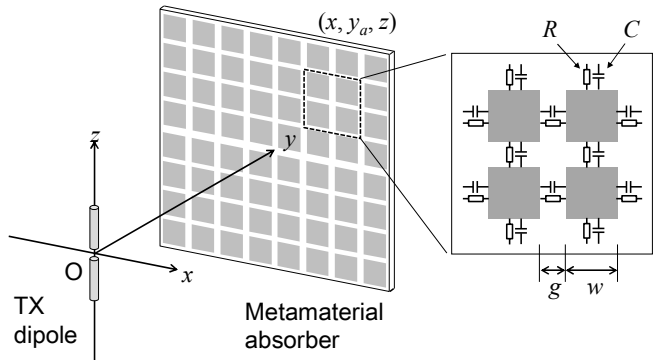


Fig. 1. Calculation model and the structure of the absorber surface.

The reflected electromagnetic field of each elementary plane wave is calculated by applying  $R^{\text{TE}}$  and  $R^{\text{TM}}$  to it. Then all the elementary plane waves are synthesized back to give the reflected field distributions on the absorber surface using (1). Similarly the transmitted (i.e., absorbed) field distributions on the absorber surface are obtained using the transmission coefficients of TE and TM waves.

### III. REFLECTED AND ABSORBED DISTRIBUTIONS

In the calculation model in Fig. 1, a spherical wave (2 GHz, 0 dBm) was radiated from the dipole, and incident on the absorber surface placed at  $y_a = 40$  cm ( $2.7\lambda$ ) from the transmitter. Only the radiation field was considered. The substrate thickness was  $h = 1.6$  mm and its relative permittivity was 4.56 ( $\tan\delta = 0$ ). On the absorber surface the size of the square metal patches and the gap between them were  $w = 10$  mm and  $g = 0.5$  mm, respectively. Surface resistors and capacitors were set as  $R = 377$  Ohms and  $C = 2.7$  pF to tune the resonance (absorption) frequency to be 2 GHz at normal incidence. Field distributions were calculated on a 12.8-m-square area on the absorber surface, which was treated as periodic by the 2-d FFT calculation in (1).

The reflection coefficients of TE and TM plane waves incident on the absorber surface are plotted in Fig. 2. Both waves are well absorbed at or near normal incidence (0 degree), whereas reflection becomes gradually large as the incident angle increases. The TM reflection is larger than the TE one over the most part of incident angles for this case.

Fig. 3 (a) shows the electric field ( $E_z$ ) distribution of the radiated spherical wave incident on the absorber surface, which represents the directionality of a transmitting vertical dipole. The reflected  $E_z$  distribution calculated by the procedure in Sec. II is plotted in Fig. 3 (b). The central portion on the  $xz$ -plane shows small reflection, because of the normal incidence. The profile along the  $z$ -axis (TM incidence) exhibits two areas with large reflection, which roughly corresponds to the incident profile in Fig. 3 (a) multiplied by the angular dependence of TM reflection in Fig. 2. The profile along the  $x$ -axis (TE incidence) shows smaller reflection but over a wider area, which can similarly be explained by the incident profile and TE reflection.

The power distribution incident on the absorber surface (the  $y$ -component of Poynting vector  $P_y$ ) is plotted in Fig. 4 (a), which represents the power directionality of the dipole transmitter. Fig. 4 (b) shows the absorbed power distribution calculated using the transmission coefficients on the absorber surface. The absorbed power becomes smaller than the incident one, in the areas with large reflection observed in Fig. 3 (b).

### IV. CONCLUSION

The reflection and absorption characteristics of a metamaterial absorber was calculated using the plane-wave expansion of a spherical wave incident on the absorber surface. It was shown that the calculation technique using (1) gives us a rigorous spatial distribution of electromagnetic field of a spherical wave radiated from a nearby RF source.

### ACKNOWLEDGMENT

Part of this work was supported by Grant-in-Aid for Scientific Research (B) (26289118) of Japan Society for the Promotion of Science (JSPS).

### REFERENCES

- [1] N. Engheta, and R. W. Ziolkowski Ed., *Metamaterials*, Wiley-IEEE Press, 2006.
- [2] S. Yagitani, K. Katsuda, M. Nojima, Y. Yoshimura, and H. Sugiura, "Imaging radio-frequency power distributions by an EBG absorber," *IEICE Trans. Commun.*, vol. E94-B, pp.2306-2315, 2011.
- [3] S. Yagitani, T. Sunahara, T. Nakagawa, D. Hiraki, Y. Yoshimura, and H. Sugiura, "Radio-frequency field measurement using thin artificial magnetic conductor absorber," *Proc. 2013 Int. Symp. on Electromagnetic Theory*, 4 pages, 2013.
- [4] S. Yagitani, I. Nagano, K. Miyamura, and I. Kimura, "Full wave calculation of ELF/VLF propagation from a dipole source located in the lower ionosphere," *Radio Sci.*, vol. 29, pp.39-54, 1994.
- [5] O. Luukkonen, F. Costa, C. R. Simovski, A. Monorchio, and S. A. Tretyakov, "A thin electromagnetic absorber for wide incidence angles and both polarizations," *IEEE Trans. Antennas Propagat.*, vol. 57, pp.3119-3125, 2009.

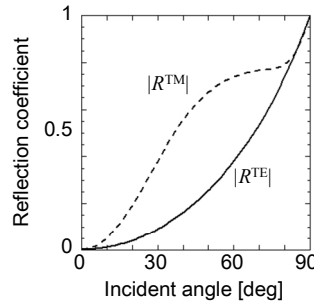


Fig. 2. Reflection coefficients from the metamaterial absorber for TE and TM incidence at 2 GHz.

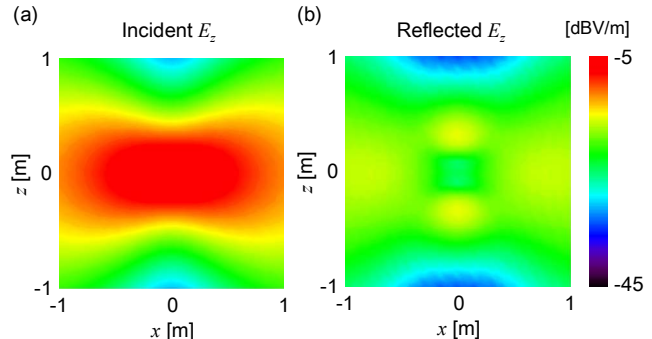


Fig. 3. Electric field ( $E_z$ ) distributions on the absorber surface: (a) for the incident wave, and (b) for the reflected wave.

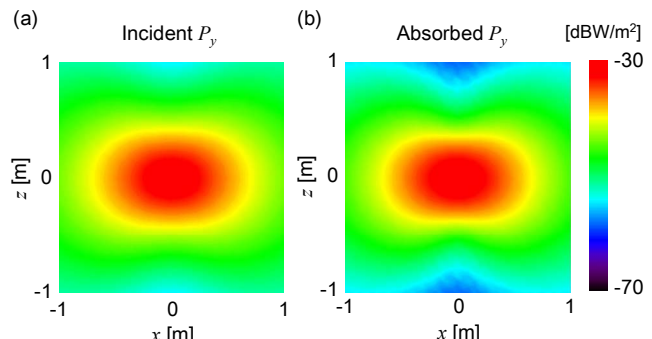


Fig. 4. Power ( $P_y$ ) distributions on the absorber surface: (a) for the incident wave, and (b) for the absorbed wave.